

Hysteresis-free and submillisecond-response polymer network liquid crystal

Yun-Han Lee, Fangwang Gou, Fenglin Peng and Shin-Tson Wu*

CREOL, The College of Optics and Photonics, University of Central Florida, Orlando, Florida 32816, USA
*swu@ucf.edu

Abstract: We demonstrate a polymer network liquid crystal (PNLC) with negligible hysteresis while keeping submillisecond response time. By doping about 1% dodecyl acrylate (C12A) into the liquid crystal/monomer precursor, both hysteresis and residual birefringence are almost completely eliminated. The operating voltage and scattering properties remain nearly intact, but the tradeoff is enhanced double relaxation. This hysteresis-free PNLC should find applications in spatial light modulators, laser beam control, and optical communications in infrared region.

©2016 Optical Society of America

OCIS codes: (160.3710) Liquid crystals; (230.3720) Liquid-crystal devices; (060.5060) Phase modulation.

References and links

1. U. Efron, *Spatial Light Modulator Technology: Materials, Devices, and Applications* (Marcel Dekker, 1994).
2. S. Quirin, D. S. Peterka, and R. Yuste, "Instantaneous three-dimensional sensing using spatial light modulator illumination with extended depth of field imaging," *Opt. Express* **21**(13), 16007–16021 (2013).
3. G. D. Love, "Wave-front correction and production of Zernike modes with a liquid-crystal spatial light modulator," *Appl. Opt.* **36**(7), 1517–1520 (1997).
4. H. Ren and S.-T. Wu, *Introduction to Adaptive Lenses* (Wiley, 2012).
5. F. Feng, I. H. White, and T. D. Wilkinson, "Free space communications with beam steering a two-electrode tapered laser diode using liquid-crystal SLM," *J. Lightwave Technol.* **31**(12), 2001–2007 (2013).
6. H. Kikuchi, J. Nishiwaki, and T. Kajiyama, "Mechanism of electro-optical switching hysteresis for (polymer/liquid crystal) composite films," *Polym. J.* **27**(12), 1246–1256 (1995).
7. L. Bouteiller and P. L. Barny, "Polymer-dispersed liquid crystals: preparation, operation and application," *Liq. Cryst.* **21**(2), 157–174 (1996).
8. Y. F. Lan, C. Y. Tsai, J. K. Lu, and N. Sugiura, "Mechanism of hysteresis in polymer-network stabilized blue phase liquid crystal," *Polym.* **54**(7), 1876–1879 (2013).
9. D. Xu, J. Yan, J. Yuan, F. Peng, Y. Chen, and S. T. Wu, "Electro-optic response of polymer-stabilized blue phase liquid crystals," *Appl. Phys. Lett.* **105**(1), 011119 (2014).
10. Y. Chen and S.-T. Wu, "Recent advances in polymer-stabilized blue phase liquid crystal materials and devices," *J. Appl. Polym. Sci.* **131**(13), 6333–6342 (2014).
11. J. Sun, Y. Chen, and S. T. Wu, "Submillisecond-response and scattering-free infrared liquid crystal phase modulators," *Opt. Express* **20**(18), 20124–20129 (2012).
12. J. Sun and S. T. Wu, "Recent advances in polymer network liquid crystal spatial light modulators," *J. Polym. Sci. Part B, Polym. Phys.* **52**(3), 183–192 (2014).
13. F. Peng, H. Chen, S. Tripathi, R. J. Twieg, and S.-T. Wu, "Fast-response infrared phase modulator based on polymer network liquid crystal," *Opt. Mater. Express* **5**(2), 265–273 (2015).
14. K. M. Chen, S. Gauza, H. Xianyu, and S. T. Wu, "Submillisecond gray-level response time of a polymer-stabilized blue-phase liquid crystal," *J. Disp. Technol.* **6**(2), 49–51 (2010).
15. F. Peng, Y. H. Lee, Z. Luo, and S.-T. Wu, "Low voltage blue phase liquid crystal for spatial light modulators," *Opt. Lett.* **40**(21), 5097–5100 (2015).

1. Introduction

Polymer network liquid crystal (PNLC) [1, 2] offers several attractive features, such as large phase change (say, 2π), sub-millisecond response time, and negligible light scattering in the infrared (IR) region. Its potential applications include spatial light modulators (SLMs) [1], adaptive optics for wave-front correction [2, 3], adaptive lens with tunable focal length [4], and beam steering [5]. However, there are still technical challenges for PNLCs, such as

relatively high operation voltage ($V_{2\pi}$), hysteresis, and double relaxation time. The high $V_{2\pi}$ originates from strong polymer network and small domain sizes. Hysteresis [6] is a common phenomenon for most polymer-stabilized liquid crystals, such as polymer-dispersed liquid crystals [7] and polymer-stabilized blue phase liquid crystals [8]. Hysteresis affects grayscale control accuracy, and should be minimized. Finally, double relaxation time involves two decay processes: a fast one followed by a slow one. In a polymer-stabilized blue phase, the fast process is governed by Kerr effect while the slower one is caused by electrostriction [9], i.e. electric field-induced polymer network deformation. For PNLCs, hysteresis and double relaxation phenomena have been observed, but not investigated in details. In recent works of polymer-stabilized blue phase liquid crystals, network modification by mono-functional and tri-functional monomers were performed to either increase response time, reduce driving voltage or suppress hysteresis [10].

In this paper, we find that by doping about 1 wt% of a mono-functional monomer (dodecyl acrylate, C12A) into the liquid crystal/di-functional monomer (RM257) precursor, the hysteresis and residual birefringence can be suppressed almost completely and operation voltage reduced slightly, but the tradeoff is increased response time, which is heavily dependent on the C12A concentration. The underlying physical mechanisms responsible for the observed phenomena are discussed.

2. Experimental

The liquid crystal host used in this experiment was HTG135200 (HCCH, China). Its physical properties are listed as follows: birefringence $\Delta n = 0.2$, dielectric anisotropy $\Delta\epsilon = 86$, and clearing temperature $T_c = 96^\circ\text{C}$. The doping concentration of di-functional monomer RM257 was 5–7 wt%, and the concentration of mono-functional monomer C12A was 0–2 wt%. Their corresponding chemical structures are plotted in Fig. 1. A 0.5-wt% photo-initiator Irgacure 819 was added to trigger the polymerization process. Each LC/monomers precursor was infiltrated into a 12- μm homogeneous cell. A 385-nm UV lamp was used to cure the sample. All samples were cured at 11°C and UV intensity $\sim 200 \text{ mW}/\text{cm}^2$ for 1 hour. The lower curing temperature and higher intensity help to reduce network domain size and thus light scattering [11]. The electro-optic properties were measured by placing the samples between crossed polarizers and a 1 kHz square-wave voltage from 0 to 100 V_{rms} was applied. A 1550-nm laser was used as the probing light source. To study hysteresis and residual birefringence, we recorded the voltage-dependent transmittance (VT) curves in the forward and backward scans. To study response (relaxation) time, we instantaneously removed the applied voltage and recorded the transient phase change. Response time is defined as phase changes from 100% to 10%.

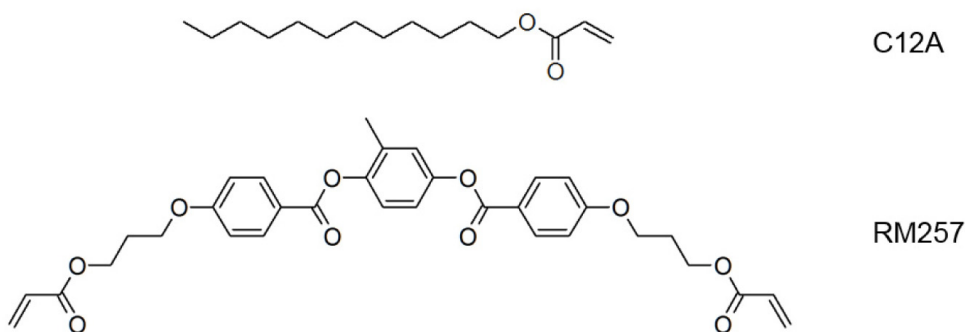


Fig. 1. The chemical structures of C12A and RM257. RM257 exhibits nematic liquid crystal phase between 70°C and 130°C while C12A does not have a mesogenic phase.

3. Results and discussion

3.1 Hysteresis

Figure 2(a) and 2(b) shows the forward and backward scans of the VT curves of two PNLC samples with 7-wt% RM257, and 6 wt% RM257 with 1 wt% C12A, respectively. The addition of merely 1% C12A suppresses the hysteresis from 3.0% to 0.0%. Here, the transmittance is normalized to that of a pure nematic LC host. Note that the transmittance reaches its maximum at about 100 V_{rms} , yet it will decrease as the voltage keeps increasing. To prevent possible electrical breakdown, we stopped at 100 V_{rms} .

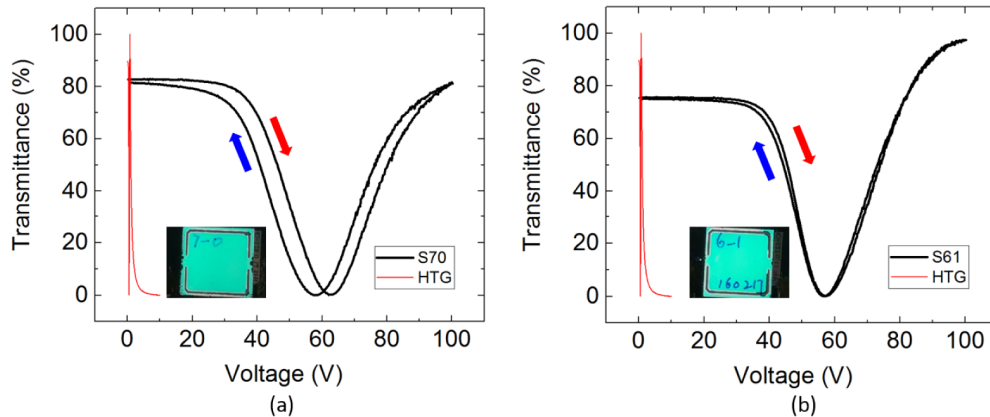


Fig. 2. Hysteresis of PNLC samples at $\lambda = 1550$ nm with (a) 7wt% RM257 without C12A and (b) 6wt% RM257 with 1wt% C12A. The red arrow indicates forward voltage scan while the blue arrow is backward. The thin red lines represent the transmittance of the LC host without polymers. Insets: the PNLC cells observed on a light table between crossed polarizers.

From Fig. 2(a), the initial transmittance and the final one at $V = 0$ do not coincide, indicating a residual Δn induced by the applied voltage. On the other hand, the sample with C12A exhibits a negligible residual Δn . For both samples (same cell gap), the operation voltage for achieving 2π phase change remains nearly the same. This suggests the interaction between the LC directors and polymer network was weakened by adding C12A. Later, we will show data to prove that the latter is the dominant factor for the reduced hysteresis. By comparing Figs. 2(a) with 2(b), we note that the initial transmittance of the PNLC sample containing C12A is $\sim 4\%$ lower than that without. This implies the LC/6%RM257/1%C12A mixture has a slightly lower Δn than LC/7%RM257. A possible explanation is that C12A does not have a mesogenic phase and its alkyl chain length is long. As a result, the molecular packing density is reduced, i.e. network is coarsened. As shown in the insets of Fig. 2, unlike the monomer M1 reported in [12] which helps to reduce operation voltage but degrades the spatial uniformity, the addition of C12A does not degrade the uniformity of the LC cells.

In experiment, we also varied the concentration of RM257 and C12A. Table 1 summarizes the measured operation voltage at π phase change ($V_{\pi, ave.}$, since V_{π} is different for forward and backward voltage scans, the average of these two is given) and the hysteresis of the PNLC with different RM257/C12A compositions. A positive correlation is found between total monomer concentration and operation voltage. This is because a higher polymer concentration leads to a smaller domain size, which in turn causes higher driving voltage, faster response time and weaker scattering. According to Ref [13], the driving voltage of a PNLC is approximately inversely proportional to the domain size. Therefore, based on the driving voltages of samples S52, S61 and S70, we find that doping C12A slightly increases the domain size. This is because C12A has a much lower viscosity than all other materials in

the precursor. Therefore, by replacing a portion of RM257 with C12A, the precursor is diluted before polymerization. The increased diffusion rate results in a larger domain size.

Another correlation found in Table 1 is that as the monomer concentration increases, hysteresis decreases. This trend is clearly manifested in samples S60, S70 and S80. It is presumably due to the more robust network at higher polymer concentration. Moreover, we find that adding 1-2% C12A helps to dramatically suppress hysteresis. However, the trade-off is increased response time. For example, the relaxation time of S70 is 212 μs , but increases to 503 μs for S61 and 1916 μs for S52. Therefore, increasing C12A concentration has pros and cons. On the positive side, it lowers the operation voltage and eliminates hysteresis almost completely, but on the negative side it increases response time dramatically. To explain these phenomena, our hypothesis is that the presence of C12A weakens the surface interaction between LC and network, which also implies to a weaker phase-mixing. As strong phase-mixing exists for the LC/RM257 composite, as a result the LC director reorientation distorts the RM257 network significantly, resulting in a noticeable hysteresis and residual Δn . While in the LC/RM257/C12A composite, the interaction between LC and RM257/C12A network is weaker, thus, the network distortion exerted by the electric field-induced LC reorientation is minimal, resulting in a negligible hysteresis but also a slower response time.

Table 1. Measured hysteresis of PNLC samples with different monomer compositions. $\lambda = 1550$ nm.

Sample	Composition (wt%)		Characteristics		
	RM257	C12A	$V_{\pi, \text{ave.}}$ (V)*	Hysteresis (%)	Relaxation time (μs)
S60	6	0	48.0	5.7	361.0
S51	5	1	46.9	1.1	1830.0
S70	7	0	66.5	3.0	212.0
S61	6	1	63.2	0.0	503.5
S52	5	2	57.0	0.2	1916.5
S80	8	0	76.9	2.0	153.6
S62	6	2	66.7	0.0	570.0

*The average voltage at π phase change of the forward and backward voltage scans.

3.2 Scattering loss

For practical applications, scattering loss of the PNLC devices should be minimized. In this part of the experiment, we removed the polarizers and investigated the scattering of PNLC in the visible and near infrared regions. In Fig. 3, we plot the measured transmittance of samples S52, S61 and S70 at 60 V_{rms} , where the maximum scattering occurs. The transmittance was normalized to a sample filled with nematic LC host only, i.e., without any polymer. To analyze the loss from scattering, we eliminate the Fabry–Pérot interference (due to ITO glass substrates) by taking the envelope of the spectra as the actual transmittance. From Fig. 3, we find that scattering increases as the C12A concentration increases, especially in the visible spectral region. Together with the reduced operation voltage shown in Table 1, we conclude that adding C12A tends to enlarge the network domain size. This is because C12A lowers the viscosity of the precursor and increases the polymer diffusion rate, which in turn leads to larger domain sizes. A larger domain size lowers the operation voltage, but increases the scattering loss and response time. At $\lambda = 1550$ nm, the scattering loss is <1% for both S70, S61 and S52.

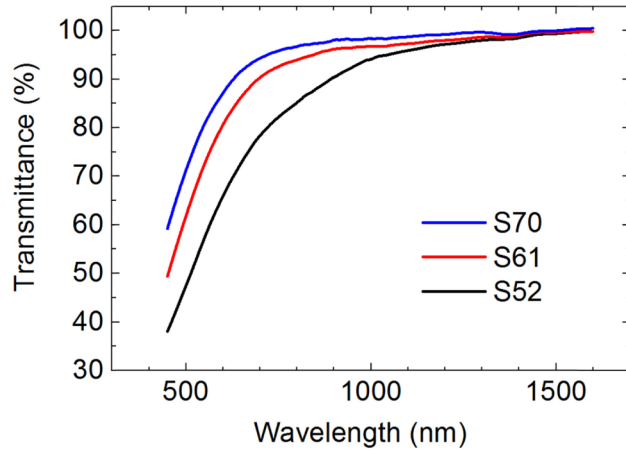


Fig. 3. Measured transmission spectra of PNLC samples S70, S61 and S52 at $60 V_{\text{rms}}$, near where the strongest scattering occurs. The relative transmittance of sample S61 is 97.8% and 99.8% at $\lambda = 1060$ and 1550 nm, respectively. Transmittance was normalized to the case when the cell was infiltrated with pure nematic host.

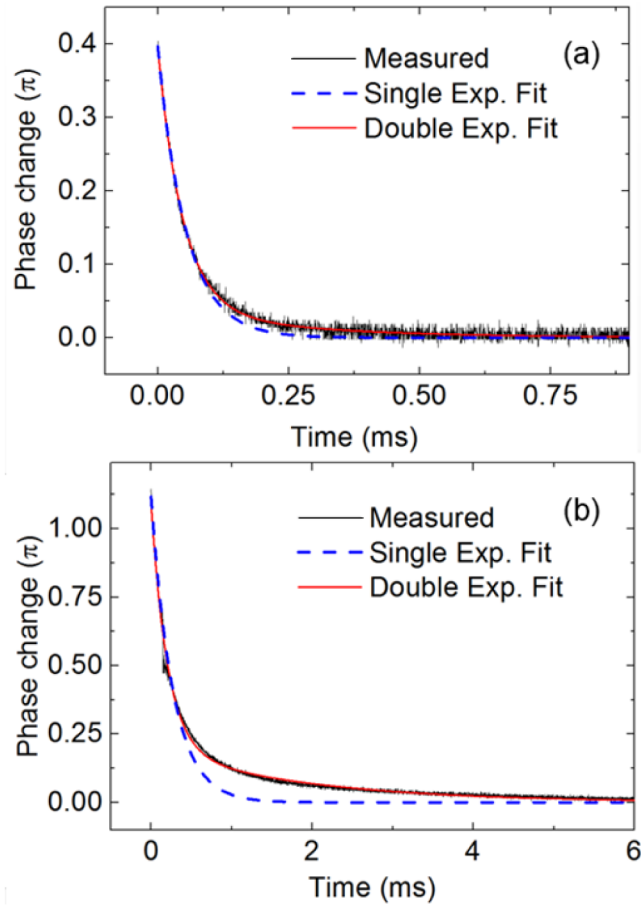


Fig. 4. The transient relaxation process of the sample (a) S70 and (b) S52 from $50 V_{\text{rms}}$ to $0 V_{\text{rms}}$ fitted with single (dashed blue lines) and double (solid red lines) relaxation curves.

3.3 Response time

Next, we compare the transient relaxation between S70 and S52 to understand the effect of C12A on the increased response time. For a polymer-stabilized system, such as blue phase, due to the complicated interaction processes between polymer network and LC domains, usually the relaxation cannot be well described by a single exponential decay but two. This phenomena is referred as double relaxation [9]. In Figs. 4(a) and 4(b), we show the transient phase change of samples S70 and S52 relaxing from 50 V_{rms} to 0 V_{rms}, respectively. For S70 (Fig. 4(a)), the single exponential decay can still fit the transient phase change process although not perfect, but not for S52 (Fig. 4(b)).

To quantitatively analyze this phenomenon, we fit the measured phase change by:

$$\Gamma(t) = A \times e^{-t/\tau_1} + B \times e^{-t/\tau_2}, \quad (1)$$

where the first term represents the fast relaxation and second term the slow relaxation, $[A, B]$ and $[\tau_1, \tau_2]$ are the corresponding weights and time constants. In experiment, samples S52, S61 and S70 were driven to different on-state voltages and released for recording the transient relaxation. The ratio defined as $A/(A + B)$ helps to quantify the degree of single relaxation. When no double relaxation presents, the second term vanishes (i.e. $B = 0$) and the ratio is equal to one. On the other hand, when a stronger double relaxation occurs, B gets larger so that $A/(A + B)$ decreases.

As Fig. 5 depicts, the $A/(A + B)$ ratio stays reasonably flat and then decreases as the electric field exceeds a threshold (E_{th}), which depends on the samples. For S70, the initial $A/(A + B)$ ratio is about 94% and $E_{th} \approx 7.5 \text{ V}/\mu\text{m}$. As the C12A concentration increases, both $A/(A + B)$ and E_{th} decrease gradually. This indicates a weaker phase-mixing such that a portion of the LC molecules were not realigned by the polymer network but followed its own free relaxation. As the electric field increases, the $A/(A + B)$ ratio gradually decreases, indicating a lower degree of phase-mixing. The decreasing trend for sample S70 is rather insignificant; yet for samples S61 and S52, an obvious decrease is found when the electric field is higher than $6.5 \text{ V}/\mu\text{m}$ and $6 \text{ V}/\mu\text{m}$, respectively. This decreased phase-mixing is attributed to a larger difference in the LC orientation and polymer in the high field region.

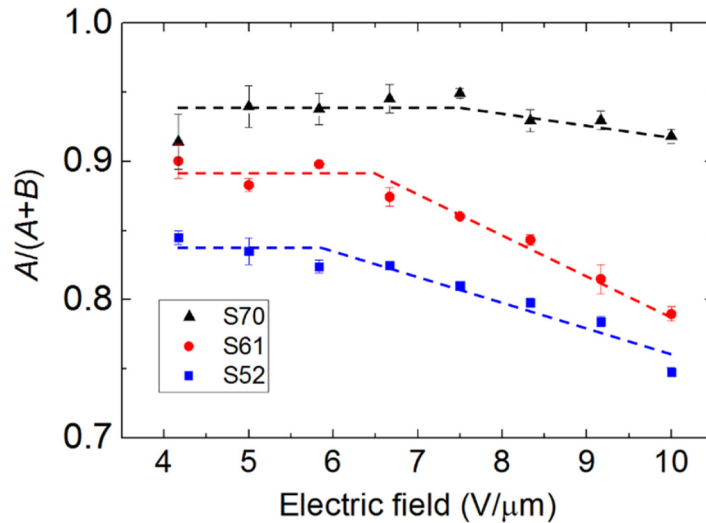


Fig. 5. The $A/(A + B)$ ratios for samples S70, S61 and S52. Only statistical errors were included. Dashed trend lines are added for visual aid.

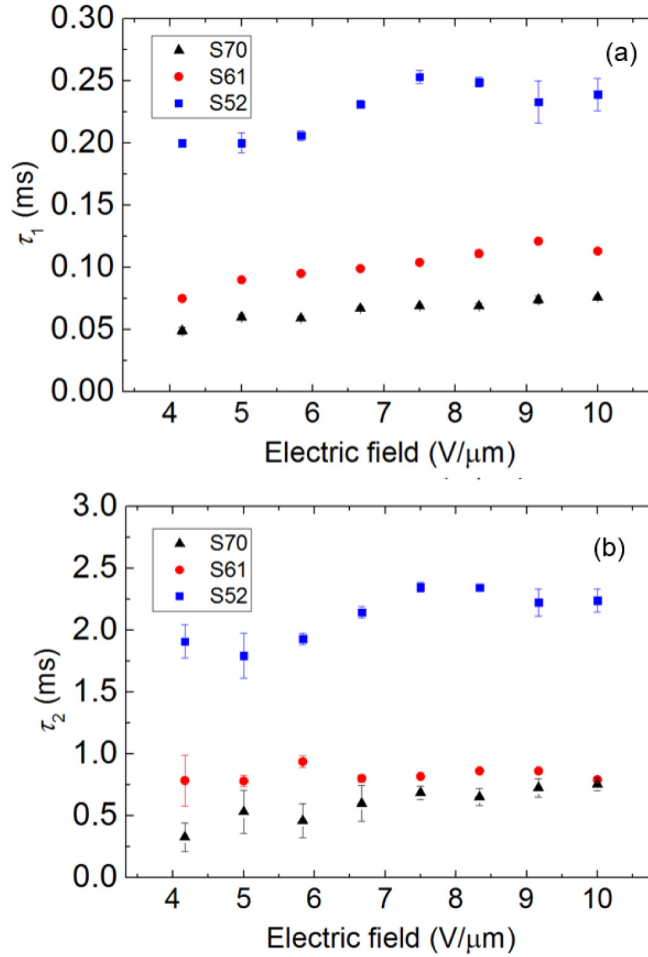


Fig. 6. (a) The extracted fast relaxation time constant (τ_1) and (b) slow relaxation time constant (τ_2) for S70, S61, and S52 PNLC samples.

In addition to A and B coefficients shown in Eq. (1), we also like to know how the C12A concentration affects the two time constants. In Fig. 6, we plot the fast and slow relaxation time constants versus electric field. For a PNLC with strong anchoring energy, its relaxation time can be approximated by [13]:

$$\tau \approx \frac{\gamma_1 d_l^2}{k_{11} \pi^2}, \quad (2)$$

where d_l represents the average domain size, γ_1 the rotational viscosity and k_{11} the splay elastic constant. However, with C12A the dramatically increased response time cannot be explained solely by the slightly increased domain size as evidenced by the increased scattering and decreased driving voltage; rather reduced anchoring energy also plays an important role. From Fig. 6(a), in the low field region τ_1 increases from 50 μs to 75 μs for PNLC samples S70 and S61, and then jumps to 200 μs for S52. As the electric field increases, τ_1 slightly increases due to the larger reorientation angle required to return to the initial state. Overall speaking, the fast relaxation time constant τ_1 increases as the C12A concentration increases, but it still stays in the sub-millisecond region. While for τ_2 shown in Fig. 6(b), it is about 10x slower than τ_1 . To keep the desirable features of PNLC, such as hysteresis-free and

low voltage while keeping sub-millisecond response time, we should consider using sample S61. For the S80 and S62 group shown in Table 1, the overall performance of S62 is still acceptable, although its operation voltage would be higher due to higher polymer concentration.

3.4 Wavelength effect

In the visible region, light scattering of PNLC is relatively strong, as depicted in Fig. 3. To eliminate light scattering, the average domain size should be controlled below 200 nm [11]. Undoubtedly, such a small domain size would dramatically increase the operation voltage. To reduce voltage while keeping scattering-free behavior and fast response time, polymer-stabilized blue phase would be a better choice [14]. Here, we concentrate on PNLC for IR SLM applications.

In Fig. 7, we compare the phase change of sample S61 at $\lambda = 1550$ nm and 1060 nm. The phase change (δ) of a PNLC SLM is related to cell gap (d), Δn , and wavelength (λ) as:

$$\delta = 2\pi d \Delta n / \lambda. \quad (3)$$

In the IR region, Δn has basically saturates; that means it remains almost the same for $\lambda = 1060$ nm and 1550 nm. From Eq. (3), the major factor affecting the phase change is λ . For a phase modulator, a 2π phase change is usually required, which corresponds to $V_{2\pi} \approx 76$ V_{rms} for $\lambda = 1060$ nm. For amplitude modulation, the corresponding π phase change occurs at $V_{\pi} \approx 53$ V_{rms} for a transmissive SLM. For a reflective SLM, such as liquid-crystal-on-silicon (LCoS), the incident light traverses twice in the LC layer [15]. Thus, its phase change is doubled and the required $V_{2\pi}$ is reduced to 26 V_{rms}. This is very close to the maximum achievable voltage for an LCoS, which is 24V. In contrast, the corresponding $V_{2\pi}$ is ~ 30 V_{rms} for $\lambda = 1550$ nm.

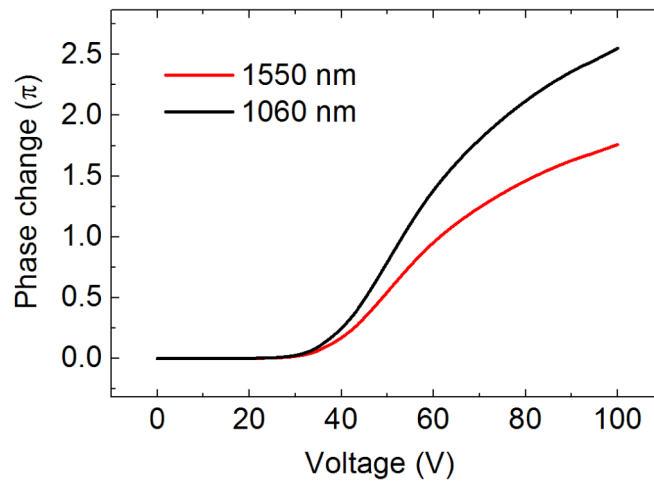


Fig. 7. The phase shift measured at $\lambda = 1550$ nm and 1060 nm of sample S61. For 1060 nm, the π and 2π phase shift occurs at 53.2 V_{rms} and 76.2 V_{rms}, respectively.

4. Conclusion

We have investigated the effects of C12A monomer on an LC/polymer composite. Interestingly, we find for PNLCs with merely 1-2 wt% C12A, several attractive features can be obtained, including dramatically suppressed hysteresis and lower operation voltage, while keeping submillisecond response time.

Acknowledgment

The authors are indebted to AFOSR for partial financial support under contract No. FA9550-14-1-0279.